

Constrained three-parameter AVO inversion and uncertainty analysis

Jonathan E. Downton and Laurence R. Lines

A colour version of this paper is available on the CREWES 2001 Research Report CD.

SUMMARY

Bayes' theorem is used to derive a three-parameter non-linear AVO inversion. Geologic constraints based on available well-control or rock-physical relationships are incorporated to help stabilize the solution. Parameter uncertainty estimates arise naturally as part of the derivation and provide estimates of the reliability of the different parameters. The resulting parameter and uncertainty estimates may be transformed to a variety of elastic and rock-physical AVO attributes popular in the literature using a transform matrix.

INTRODUCTION

The elastic parameters may be estimated, using a linearized approximation of the Zoeppritz equation such as Aki and Richards (1980),

$$r(\theta) = \frac{1}{2} (1 - 4\gamma^2 \sin^2 \theta) \frac{\Delta\rho}{\rho} + \frac{1}{2} \frac{\Delta\alpha}{\alpha} \frac{1}{\cos^2 \theta} - 4\gamma^2 \left(\frac{\Delta\beta}{\beta} \right) \sin^2 \theta, \quad (1)$$

where r is the angle dependent reflectivity. The parameters α , β , ρ , γ respectively are the average p-wave velocity, s-wave velocity, density and the ratio of S-velocity to P-velocity across the interface. The variable θ is the average angle-of-incidence and $\Delta\alpha$, $\Delta\beta$, $\Delta\rho$ are the change in p-wave velocity, s-wave velocity, and density. Equation (1) may be written in matrix form $\mathbf{G}\mathbf{m}=\mathbf{d}$ where \mathbf{G} is the linear operator, \mathbf{m} , the unknown parameter vector containing the velocity and density reflectivity $[\Delta\alpha/\alpha, \Delta\beta/\beta, \Delta\rho/\rho]^T$ and \mathbf{d} the input data vector (offset-dependent reflectivity).

In practice, equation (1) is rarely inverted. For conventional acquisition geometries and noise levels, equation (1) is ill-conditioned. That is, a small amount of noise will result in large parameter deviations. This problem becomes worse as the range of angles used in the inversion becomes smaller. Various authors (Shuey (1985), Smith and Gidlow (1987), and Fatti et al (1994), among others) rearrange equation (1) to solve for other parameterizations. In implementing these schemes, hard constraints are usually implemented either explicitly or implicitly to improve the stability of the problem. Smith and Gidlow (1987) use the Gardner equation (Gardner et al., 1973) to remove the density reflectivity, thus improving the stability of the problem. The Shuey and Fatti equations are generally both solved using only the first two terms, implicitly constraining the third term's reflectivity to zero.

Rather than using hard constraints, this paper uses soft constraints from the well control or from rock-physical relationships. The degree to which the constraint

influences the solution is dependent on the signal-to-noise level of the data and the acquisition geometry. In the case of good signal-to-noise data and a large angle range, the constraints only influence the solution in a minor way. Under these conditions, the density reflectivity might be reliably solved for. For poor signal-to-noise-ratio data or a data with limited angle range, the constraints will dominate the solution. Parameter estimates will have greater uncertainty and quality control displays must be relied upon to determine if the estimate is useable (Downton et al, 2000)

Bayes' theorem provides a convenient theoretical framework to do this. This paper first reviews Bayes' theorem, the Likelihood function, and the prior constraints. It is shown how well control or rock physical relationships can be used to construct a prior probability function. Then, by combining the Likelihood function and the *a priori* probability function, a non-linear inversion algorithm is derived. Next, the reliability of the estimates is discussed. It is shown that the parameter estimate and uncertainty can be transformed to other AVO attributes that might be more suitable to interpret the data. Lastly, the algorithm is demonstrated on both synthetic and real seismic data.

THEORY

Bayesian Inversion

Bayes' theorem provides a theoretical framework to make probabilistic estimates of the unknown parameters \mathbf{m} from uncertain data and *a priori* information. The resulting probabilistic parameter estimates are called the Posterior Probability Distribution function (PDF). The PDF written as $P(\mathbf{m}|\mathbf{d},I)$ symbolically indicates the probability of the parameter vector, \mathbf{m} , given the data vector \mathbf{d} , (offset-dependent reflectivity) and information, I . Bayes' theorem

$$P(\mathbf{m} | \mathbf{d}, I) = \frac{P(\mathbf{d} | \mathbf{m}, I)P(\mathbf{m} | I)}{P(\mathbf{d} | I)}, \quad (2)$$

calculates the PDF from the likelihood function $P(\mathbf{d}|\mathbf{m},I)$ and *a priori* probability function $P(\mathbf{m}|I)$. The denominator $P(\mathbf{d}|I)$ is a normalization function which may be ignored if only the shape of the PDF is of interest.

$$P(\mathbf{m} | \mathbf{d}, I) = P(\mathbf{d} | \mathbf{m}, I)P(\mathbf{m} | I). \quad (3)$$

The most likely estimate occurs at the maximum of the PDF. The uncertainty of the parameter estimate is proportional to the width of the PDF.

Likelihood function

If we assume uniform uncorrelated Gaussian noise then the likelihood function may be written as (Sivia, 1996)

$$P(\mathbf{d} | \mathbf{m}, I) \propto \sigma^{-N} \exp \left[-\frac{\sum_{k=1}^N \left(\sum_{i=1}^M G_{ki} m_i - d_k \right)^2}{2\sigma^2} \right], \quad (4)$$

where σ^2 is the variance of the noise. In the case of uniform priors, Bayesian inversion is equivalent to maximum likelihood inversion.

For AVO inversion, because of the small number of parameters solved for, it is possible to visualize the PDF. If the parameter vector \mathbf{m} had only one element, the PDF would be a Gaussian function. If the parameter vector \mathbf{m} had two elements, the PDF would be a bivariate Gaussian function and an equiprobable solution would be an ellipse. For the case of AVO inversion, where there are 3 parameters, the PDF is a multivariate Gaussian function where an equiprobable solution is an ellipsoid. Typically the ellipsoid is quite elongated along the density reflectivity axis. The solutions are non-physical when the reflectivity is greater than 1.

A priori constraints

One way to reduce the uncertainty is to impose constraints on the solution. For example, non-physical solutions can be excluded from the solution space. This can be written in terms of a probability distribution where physical solutions are equiprobable and non-physical solutions given zero probability.

It is not necessarily desirable to assign uniform probabilities over the range of physically valid reflectivity. The stratigraphic sequence is a result of cyclic geologic processes that result in reflectivity probability functions, which may be reasonably described by common probability functions. The normal distribution was found to reasonably describe the statistics of logs for this work in Western Canada. Other probability functions may be used if appropriate, but for this paper the normal probability function is used. The joint probability distribution for the P-velocity, S-velocity and density reflectivity is the multi-variate Gaussian distribution that is parameterized by a covariance matrix. The diagonal elements of the covariance matrix are the variances of the P-velocity, S-velocity and density reflectivity. The off-diagonal elements describe how correlated the P-velocity, S-velocity and density reflectivity are.

From rock physics studies it has been empirically observed that the P-velocity, S-velocity and density are correlated. The mudrock relationship (Castagna et al, 1985) provides a relationship linking P-velocity and S-velocity reflectivity, $R_{vs}=mR_{vp}$. The Gardner relationship (Gardner et al, 1973) provides a relationship between the P-velocity and density reflectivity, $R_d=gR_{vp}$. Potter et al. (1998) observed a similar relationship between S-velocity and density reflectivity, $R_d=fR_{vs}$. These parameters and their correlation coefficients r_1 , r_2 and r_3 can be calculated from the local well control. From this the parameter covariance matrix C_m , which defines the multivariate Gaussian distribution can be constructed.

$$\begin{bmatrix} \sigma^2_{R_{Vp}} & \sigma_{R_{Vp}R_{Vs}} & \sigma_{R_{Vp}R_{den}} \\ \sigma_{R_{Vp}R_{Vs}} & \sigma^2_{R_{Vs}} & \sigma_{R_{Vs}R_{den}} \\ \sigma_{R_{Vp}R_{den}} & \sigma_{R_{Vs}R_{den}} & \sigma^2_{R_{den}} \end{bmatrix} = \sigma^2_{R_{Vp}} \begin{bmatrix} 1 & m & g \\ m & \frac{m}{r_1^2} & f \\ g & f & \frac{g}{r_2^2} \end{bmatrix}. \quad (5)$$

In practice, it is more efficient to calculate this directly from the sample statistics, but the proceeding analysis provides physical significance to each of the terms in the parameter covariance matrix. In addition, in areas with limited well-control or missing information, published values may be used to help construct the covariance matrix.

The resulting *a priori* probability function is the multi-variate Gaussian probability function

$$P(\mathbf{m} | I) \propto \exp\left[-\frac{1}{2} \mathbf{m}^T \frac{\mathbf{C}_m^{-1}}{\eta^2} \mathbf{m}\right], \quad (6)$$

where η is a global scale factor to account for the arbitrary scaling of the seismic data.

Nonlinear inversion

The Likelihood function (equation 4) may be combined with the *a priori* probability function (equation 6) using Bayes' Theorem (equation 3). Since there is no explicit interest in the variance σ or the scalar η , both are marginalized (Sivia, 1996). The most likely solution can then be found by finding where the probability function is stationary. This involves taking the partial derivatives with respect to each parameter, setting the result to zero and solving the set of simultaneous equations. This results in the nonlinear equation

$$\mathbf{m} = \left[\mathbf{G}^T \mathbf{G} + \frac{2\boldsymbol{\varepsilon}^T \boldsymbol{\varepsilon}}{(N-1)Q} \mathbf{C}_m^{-1} \right]^{-1} \mathbf{G}^T \mathbf{d}, \quad (7)$$

where $\boldsymbol{\varepsilon} = \mathbf{G}\mathbf{m} - \mathbf{d}$ and $Q = \mathbf{m}^T \mathbf{C}_m^{-1} \mathbf{m}$. The equation is weakly nonlinear and can be solved in an iterative fashion using Newton-Raphson. The term $\boldsymbol{\varepsilon}^T \boldsymbol{\varepsilon}$ is an estimate of the RMS energy of the noise and Q the RMS energy of the signal. The ratio is therefore an estimate of the N/S ratio. The ratio acts as a weighting factor determining how much the prior constraints influence the solution. If the S/N is large, then the weighting factor is small and the constraints add little to the solution and vice versa.

Uncertainty analysis

The uncertainty of the parameter estimate is related to the width of the distribution. This can be calculated from the 2nd derivative evaluated at the parameter estimate.

With the assumption of uniform uncorrelated Gaussian noise the uncertainty is described by the covariance matrix

$$\mathbf{C}_d = \left[\mathbf{G}^T \mathbf{G} + \frac{2\boldsymbol{\varepsilon}^T \boldsymbol{\varepsilon}}{(N-1)Q} \mathbf{C}_m^{-1} \right]^{-1} \quad (8)$$

The diagonal of the covariance matrix represents the variance of each parameter estimate. The off-diagonal element represents the degree of correlation between the errors (Downton et al., 2000).

It is also important to understand how much the constraints are influencing the solution. The uncertainty can also be calculated if the constraints were not included. The ratio of these two uncertainty estimates give a sense of how much of the solution is coming from the data and how much from prior knowledge. To make accurate predictions about the subsurface the parameter estimate of interest should be largely coming from the data.

Transform matrix

In this paper the P-velocity, S-velocity, and density reflectivity are estimated. In the literature, equation (1) has been rearranged to solve for impedance reflectivity (Fatti et al, 1994), Lamé reflectivity (Gray et al, 1999), geometric parameters A,B,C (Shuey, 1985), and many others. This being the case, it is simple to construct a transform matrix to transform from velocity reflectivity to any of these other attributes $\mathbf{m}' = \mathbf{T}\mathbf{m}$ where \mathbf{T} is the transform matrix and \mathbf{m}' is the new parameter set. The parameter uncertainty covariance matrix can also be transformed by $\mathbf{C}_m' = \mathbf{T}\mathbf{C}_m\mathbf{T}^T$. In this way different AVO attributes can be examined to see how they show off some particular geologic feature or anomaly. An attribute can be selected which highlights the objective the best. Of equal importance, the reliability of each of these attributes can also be examined to understand whether the anomaly is reliable or an artifact due to the noise.

EXAMPLES

Synthetic example

The method has been tested on both synthetic and real data. The synthetic data was generated based on two wells from Western Canada. Synthetic gathers were generated with a variety of different acquisition geometries to understand how the inversion would react to changes in fold, angle range, and signal-to-noise. The constraints were constructed based on a composite of logs in each area. The results of the constrained inversion were transformed to impedance reflectivity and compared to the corresponding zero-offset reflectivity attributes.

In order to get a reliable estimate of the density reflectivity, we need to have seismic data with good signal-to-noise and large incidence angle range. Figure 1 shows the AVO inversion for the angle range of 0 to 45 degrees, for a synthetic

gather with a signal-to-noise ratio of 8. With this large angle range and good S/N ratio, reliable estimates of the density reflectivity are possible. Note that in this example the density and velocity are uncorrelated. Figure 2 shows the results of the AVO inversion, but on a gather with a signal-to-noise ratio of $\frac{1}{4}$. In this case, the estimate of the density reflectivity does not correlate well with the actual reflectivity. The estimate is coming primarily from the constraints.

Data Example

The inversion so far has been run on seven different seismic lines. Only one line had sufficient angle range and signal-to-noise ratio to give a geologically significant density reflectivity estimate (Figure 3). The zone of interest is the bright spot around 0.72 seconds. Well A is a non-economic gas well which encountered low gas saturations, whereas wells C and E encountered economic gas. The porosity and thickness of the sands in all the wells are equivalent. The P-impedance and fluid stack (not shown) give the same response for all the wells. Note that the density section gives a brighter response for the economic gas as expected.

Figure 4 shows the standard deviation and the influence of the constraints on the density reflectivity estimated. Around CDP 2000 the seismic line went through muskeg, resulting in poorer quality records. The standard deviation is much larger in this area. Because of the poorer S/N ratio, the constraints are weighted more in the solution. This influence shows in the ratio of constrained to unconstrained uncertainty (Figure 4, bottom panel). However, for most of the zone of interest, the solution is largely coming from the data. This, combined with the good geologic correlation with the well control, suggests the density section is reasonable.

CONCLUSIONS

We have demonstrated a three-parameter AVO inversion using soft constraints. The degree to which the constraints influence the solution is a function of the signal-to-noise ratio of the data. The constraints preferably should be calculated from local well control. If local well control is not available, values from the literature may be used. Velocity and density reflectivity are solved for, but can be transformed subsequently to virtually any other AVO attribute. Parameter uncertainty estimates are provided as part of the derivation and should be examined to determine the significance and reliability of a particular AVO attribute. This is particularly true of the density reflectivity. Density reflectivity may be reliably estimated for data with little noise and large angle range.

The results of the three-term constrained AVO inversion are equivalent to the Smith and Gidlow AVO inversion if the *a priori* constraints define the density reflectivity as a linear function of the P-velocity reflectivity. Similarly, the results of the inversion are equivalent to the two-term Fatti equation (Fatti et al, 1994), if the *a priori* information specifies the density reflectivity is zero. Lastly the three-term AVO inversion is equivalent to the two-term Shuey equation with the *a priori* constraint that the velocity reflectivity is zero. By choosing constraints based on local well control, honouring known rock physical relationships, and weighting the constraints

based on the needs of the data, the results of the constrained 3 parameter AVO inversion should be more accurate than the aforementioned methods.

ACKNOWLEDGEMENTS

The authors thank AOSTRA and the CREWES sponsors for funding this research. In addition, the authors thank Yongyi Li and Yong Xu of Scott Pickford for their helpful suggestions.

REFERENCES

- Aki, K. and Richards P.G., 1980, Quantitative seismology: theory and methods: W.H. Freeman and Co.
- Castagna, J.P, Batzle, M.L., and Eastwood, R.L., 1985, Relationships between compressional-wave and shear wave velocities in clastic silicate rocks: 50, 571-581
- Downton J., Lines, L.R., Goodway, W., Xu, Y., and Li, Y, 2000, Predicting the statistical properties of the fluid stack: 70th annual international SEG meeting, expanded abstracts
- Fatti, J.L., Smith, G.C., Vail, P.J., Strauss, P.J., and Levitt, P.R., 1994, Detection of gas in sandstone reservoirs using AVO analysis: A 3-D seismic case history using the Geostack technique, *Geophysics*, 59, 1362-1376
- Gardner, G.H.F., Gardner, L.W. and Gregory, A.R., 1974, Formation velocity and density - The diagnostic basics for stratigraphic traps: *Geophysics*, **39**, no. 06, 770-780.
- Gray, D., Goodway, B. and Chen, T., 1999, Bridging the Gap - Using AVO to Detect Changes in Fundamental Elastic Constants: 61st Mtg. Eur. Assoc. Expl Geophys., Extended Abstracts, European Association Of Geophysical Exploration, Session: 6050.
- Potter, C.C., Dey, A.K., Stewart, R..R., 1998, Density prediction using P- and S-wave sonic velocities: Geotriad, 1998 CSPG, CSEG, CWLS Joint convention, p 320
- Shuey, R.T. 1985, A simplification of the Zoeppritz equations: *Geophysics*, 50, 609-614
- Sivia, D. S., 1996, *Data Analysis, A Bayesian tutorial*: Oxford university press
- Smith, G.C., and Gidlow, P.M., 1987, Weighted stacking for rock property estimation and detection of gas; *Geophysical Prospecting*, 35, 993-1014

3 term AVO inversion 0-45 degrees, S/N=8

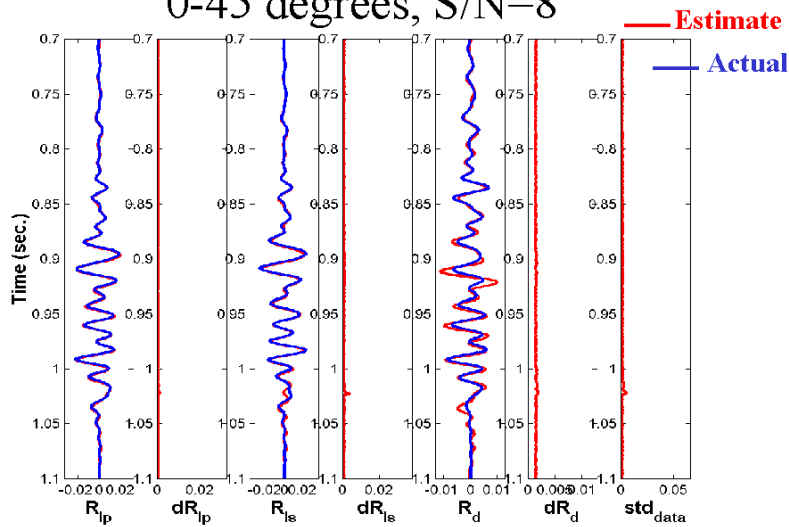


FIG 1. Results of AVO inversion from 0 to 45 degrees for P-impedance, S-impedance and density reflectivity attributes on a gather with a S/N=8. The estimate is in red and the actual reflectivity in blue. The estimated standard deviation of the P-impedance reflectivity is labelled dR_{ip} , S-impedance reflectivity is labelled dR_{is} and density reflectivity is labelled dR_d and std_{data} is the standard deviation of the prestack data.

3 term AVO inversion 0-45 degrees, S/N=1/4

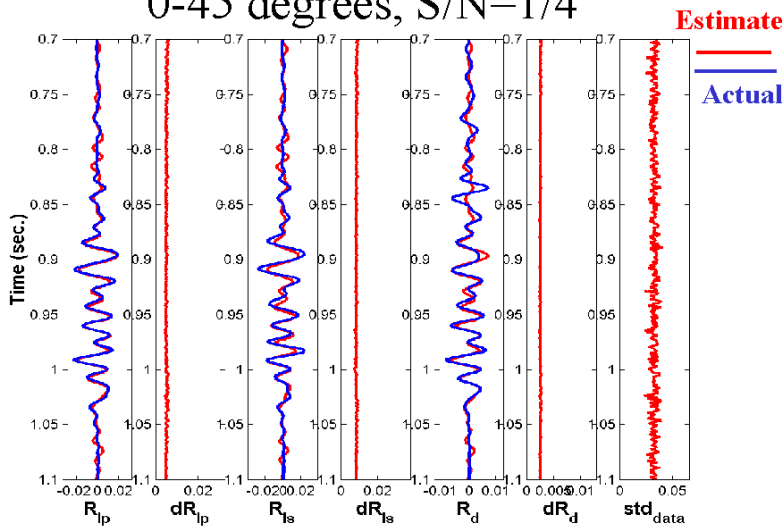


Fig. 2. Results of AVO inversion from 0 to 45 degrees for P-impedance, S-impedance and density reflectivity attributes on a gather with a S/N=1/4. The estimate is in red and the actual reflectivity in blue. The estimated standard deviation of the P-impedance reflectivity is labelled dR_{ip} , S-impedance reflectivity is labelled dR_{is} and density reflectivity is labelled dR_d and std_{data} is the standard deviation of the prestack data.

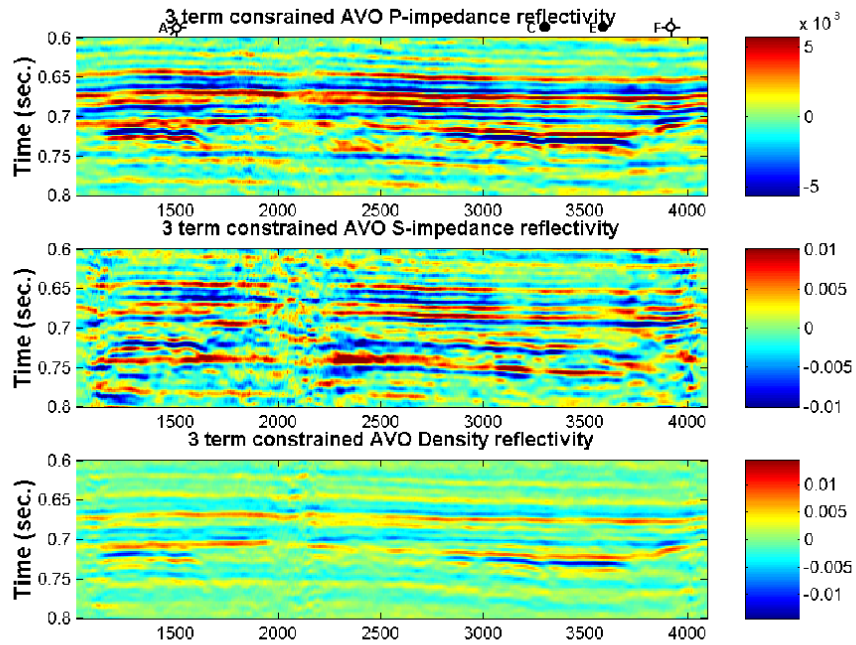


FIG. 3. P-impedance, S-impedance, and density reflectivity attribute inversions over producing and non-economic gas fields. Note that it is possible to differentiate on the density section the low gas saturation gas well (Well A) from the economic gas wells (Well C and E).

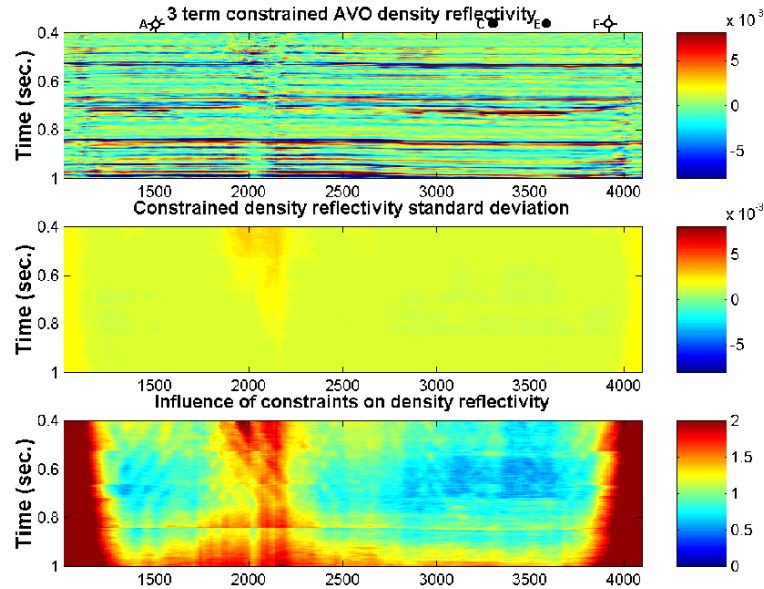


FIG. 4. The density reflectivity and related quality control sections. The standard deviation of the density (middle panel) is considerably smaller than the density reflectivity at the zone of interest. The ratio of the unconstrained to constrained uncertainty (bottom panel) shows the influence of the constraints on the solution. Where this ratio is high, the constraints are dominating the solution. This occurs when the S/N is poor or the range of angles available for the inversion is limited.